Tracking the budget of Nb and Ta in the continental crust

Matthias G. Barth [*], William F. McDonough, Roberta L. Rudnick

Department of Earth and Planetary Sciences, Harvard University, 20 Oxford Street, Cambridge, MA 02138, USA

Abstract

High precision trace element data are reported for representative samples of the upper continental crust: 11 loess samples and 22 shale samples (PAAS) previously used by Taylor and McLennan to define the rare earth element (REE) content of the upper crust. Our results confirm the REE concentrations of Taylor and McLennan's [Taylor, S.R., McLennan, S.M., 1985. The continental crust: its composition and evolution. Blackwell, Oxford, 312 pp.] estimate of the upper continental crust but suggest substantial revisions for Nb and Ta, in agreement with recent work of Plank and Langmuir [Plank, T., Langmuir, C.H., 1998. The chemical composition of subducting sediment and its consequences for the crust and mantle. Chem. Geol. 145, 325–394.]. From our data, the upper continental crust has average Nb = 11.5 ± 2.6 ppm (instead of 25 ppm) and Ta = 0.92 ± 0.12 ppm (instead of 2.2 ppm), which translates into a bulk crust Nb = 8 ppm, Ta = 0.7 ppm, La/Nb = 2.2, and Nb/Ta = 12–13. These revisions confirm the crustal subchondritic Nb/Ta and superchondritic La/Nb ratios and reinforce the observation that the continental crust and the Depleted Mantle are not strictly complementary: an additional Nb- and Ta-rich reservoir having superchondritic Nb/Ta is required to balance the Silicate Earth. Using the continental crust's La/Nb ratio to estimate the proportions of crustal growth in convergent margin and intraplate settings, we suggest a plume contribution of only between 5 and 20% to the continents, even lower than previous estimates. © 2000 Elsevier Science B.V. All rights reserved.

Keywords: Composition of continental crust; Loess; Shale; Niobium; Tantalum

1. Introduction

The refractory lithophile elements Nb, Ta, and rare earth elements (REE) are assumed to be in chondritic proportions in the Silicate Earth. Nb and Ta are identical in charge and nearly identical in size and hence show strongly coherent geochemical behavior. For these reasons, fractionation of Nb and Ta from REE has provided crucial constraints on crust–mantle differentiation and crustal growth processes (Hofmann et al., 1986; Rudnick, 1995).

Although the continental crust comprises only a small fraction of the mass of the earth, a significant portion of the Earth's incompatible trace elements resides in the continents. Therefore, defining the crust's composition is crucial for understanding mass balance of these elements in the Earth. Specifically, it is well established that the continental crust is depleted in Nb and Ta relative to other highly incompatible elements such as La. Likewise, average

---

[*] Corresponding author. Tel.: +1-617-496-4356; fax: +1-617-496-0434; e-mail: barth@eps.harvard.edu

MORB is depleted in Nb and Ta relative to La and one can therefore assume that the Depleted Mantle (i.e., MORB source) shows a similar depletion, given that Nb and Ta are more incompatible than La during MORB genesis (Hofmann, 1988; Sun and McDonough, 1989). The superchondritic La/Nb values for the continental crust (1.3–2.2, Rudnick and Fountain, 1995; and references therein) and for average MORB (1.1–1.3, Hofmann, 1988; Sun and McDonough, 1989) demonstrate that these are not complementary silicate reservoirs (Sun and McDonough, 1989; McDonough, 1991). Although the continental lithospheric mantle has subchondritic La/Nb, its low La and Nb concentrations imply that the continental lithospheric mantle is not an important Nb-bearing reservoir within the Earth (McDonough, 1991). Thus, other Nb- and Ta-rich reservoirs are needed to balance the Silicate Earth.

It is also debated whether Nb and Ta are fractionated from each other during crust–mantle differentiation. The primitive mantle has a chondritic Nb/Ta ratio of 17.4 ± 0.5, and the Depleted Mantle a subchondritic ratio of 15.5 ± 1 (Jochum et al., 1997). The crustal Nb/Ta values of about 11–12 (Taylor and McLennan, 1985; Rudnick and Fountain, 1995) are less well established due to the lack of high-quality data for Nb and Ta on representative crustal samples.

Finally, determining the concentrations of high-field strength elements (HFSE) in the continental crust can be important for establishing the style of crustal growth. The depletion of Nb relative to light REE, as seen in the crust, is indicative of crustal growth at convergent margins rather than intraplate settings, but determining the proportions of these two end members is critically dependent on defining the La/Nb ratio of the crust.

Because Nb, Ta and REE are concentrated in the upper continental crust (UCC) relative to the lower crust, determining its composition is critical for understanding the bulk crust composition. Fortunately, the upper crust is accessible to large-scale sampling through the processes of sedimentation. Previous studies have demonstrated that the average composition of UCC can be obtained for elements that are insoluble in water from aeolian deposits as well as from fine-grained clastic sediments (Nance and Taylor, 1976; Taylor et al., 1983; Gallet et al., 1998).

2. Samples of the upper continental crust

To address the question of Nb and Ta abundances in the continental crust we have undertaken precise trace element measurements on a fundamental suite of representative samples that were previously analyzed by Taylor and colleagues to estimate the REE content of the UCC. The suite consists of 11 loess samples from Banks Peninsula, New Zealand, Kansas and Iowa, USA, and Kaiserstuhl, Germany (Taylor et al., 1983) and 22 shales (post-Archean average Australian shale (PAAS), Nance and Taylor, 1976; McLennan, 1989).

Because loess is an aeolian deposit, derived from glacial outwash and from desert environments (e.g., Smalley and Vita-Finzi, 1968; Flint, 1971), weathering has a relatively small effect on its chemistry. However, major element systematics imply that loess deposits have experienced at least one cycle of aquatic sedimentary differentiation processes (Gallet et al., 1998). The very nature of the aeolian transport mechanism also ensures that a geographically widespread area will be sampled.

In contrast, shales are formed by more complex processes compared with the simple abrasion process experienced during glacial erosion, and they generally show higher degrees of weathering than loess. However, elements with low solubility in natural waters (e.g., Nb, Ta and REE) are considered immobile. Consequently, it is likely that these elements are transferred nearly quantitatively from the site of weathering into clastic sediments. Although REE patterns in loess and shales are parallel to upper crustal patterns, they overestimate the absolute abundances by about 20% due to the presence of sediments with much lower REE concentrations, such as sandstones, carbonates, and evaporites (Taylor and McLennan, 1985).

3. Analytical methods

Nb, Ta, REE, and other trace elements were determined by inductively coupled plasma-mass spectrometry (ICP-MS). The principal difficulties of measuring HFSE in dissolved rocks are incomplete acid digestion, solution instability, and memory ef-

fects. These obstacles can cause poor precision (e.g., Jenner et al., 1990; Xie et al., 1994) and lower concentrations compared with other techniques that do not require sample dissolution, such as spark source mass spectrometry (SSMS), X-ray fluorescence (XRF), and INAA (e.g., Hall and Plant, 1992; Totland et al., 1992). The procedure described below was developed to overcome these analytical problems.

Samples were dissolved in a mixture of ultrapure, concentrated HF-HNO$_3$ and then spiked with a mixed multi-element/enriched isotope internal standard solution prior to analysis, following the technique of Eggins et al. (1997). Complete dissolution of the samples was ensured by the use of conventional oven bombs. The HFSE, especially Ta, have a strong tendency for precipitation or adsorption on container walls. Therefore, analyte stability was enhanced by addition of dilute HF to the solutions (see discussion

in Münker, 1998). Dilution of the samples in 2% HNO$_3$ and 0.1% HF gave satisfactory results for HFSE in the reference materials AGV-1 and GSP-1 (Table 1). The latter standard was chosen to demonstrate the efficiency of bomb dissolutions. Our Zr value is high compared to that in Govindaraju (1994) (628 vs. 530 ppm), but overlaps the rather large range of Zr concentrations determined by Owen and Faure (1974) by isotope dilution. This range, coupled with visible particles in our USGS powder aliquots (split 27, position 20), suggests sample heterogeneity with respect to zircons. Note that the Nb and Ta abundances are the same as reported by Govindaraju (1994).

Analyses were performed on a Fisons (VG Elemental) PQ II + in pulse counting mode (three points per peak). Dwell time and quadrupole settling time were set to 10 ms and 5 ms, respectively. Sensitivity of the instrument was on average ~50

Table 1
Blank levels and USGS reference standards AGV-1 and GSP-1 analyzed by ICP-MS

	AGV-1 reference value	AGV-1 ppm, $n = 11$	RSD, %	GSP-1 reference value	GSP-1 ppm, $n = 11$	RSD, %	Blank ppb, $n = 8$	detection limits, ppb 3σ
Ga	21.2	20.1	6.0	23	22.4	3.9	0.017	0.017
Sr	660	666	11.5	234	194	5.4	0.240	0.373
Y	19.5	19.9	8.6	27	26.8	3.8	0.005	0.006
Zr	230	241	7.3	595	628	2.8	0.082	0.107
Nb	14.5	14.5	4.5	27.9	26.8	3.5	0.005	0.020
Cs	1.25	1.2	9.8	1.02	1.0	7.0	0.001	0.002
Ba	1210	1203	9.3	1310	1317	2.8	0.854	5.349
La	39	38.7	13.6	184	189	2.6	0.006	0.008
Ce	69	68.4	3.9	399	448	4.6	0.010	0.017
Pr	8	8.27	7.3	52	57.9	3.4	0.002	0.003
Nd	32	31.2	7.1	196	201	3.3	0.008	0.018
Sm	5.9	5.62	4.8	26.3	26.3	5.5	0.011	0.009
Eu	1.55	1.64	4.9	2.33	2.31	3.9	0.001	0.001
Gd	4.7	4.50	5.2	12.1	12.6	4.7	0.001	0.003
Tb	0.7	0.68	7.5	1.34	1.46	4.1	0.000	0.001
Dy	3.8	3.59	6.0	5.5	6.59	4.4	0.001	0.003
Ho	0.7	0.68	3.8	1.01	0.98	2.8	0.000	0.001
Er	1.9	1.92	4.2	2.7	2.57	3.0	0.001	0.002
Yb	1.75	1.62	3.7	1.7	1.74	3.4	0.001	0.002
Lu	0.27	0.257	5.6	0.214	0.234	5.4	0.001	0.001
Hf	5.17	5.32	6.3	15.5	16.3	3.5	0.003	0.005
Ta	0.90	0.90	3.2	0.97	0.93	4.4	0.004	0.007
Th	6.5	6.25	3.2	106	109	5.6	0.002	0.004
U	1.90	1.92	3.5	2.54	2.51	4.5	0.001	0.001

The values for both AGV-1 and GSP-1 are averages of 11 repeat analyses of four digestions. The RSD is the relative standard deviation in percent. The blank values are the average of eight repeated analyses of four different procedural blanks. Recommended values from Govindaraju (1994) except Zr in GSP-1 (595 ± 21 ppm) which is from Owen and Faure (1974).

Table 2
Trace element concentrations (in ppm) of loess and shales determined by ICP-MS

| | Banks Peninsula | | | | | Kansas | | | Iowa | Kaiserstuhl | |
	BP-1	BP-2	BP-3	BP-4	BP-5	CY-4a-A	CY-4a-B	CY-4a-C		1	2
Ga	16.6	16.7	17.3	16.7	15.6	11.3	12.0	12.4	12.3	6.9	6.8
Sr	271	304	300	276	300	170	192	216	139	389	300
Y	29.1	26.5	33.1	26.3	26.3	26.4	32.0	31.4	29.9	26.5	28.8
Zr	437	410	576	401	425	645	645	664	445	303	293
Nb	11.6	11.2	17.6	11.8	11.4	14.0	15.7	15.1	15.1	10.0	9.5
Cs	4.4	4.5	4.0	4.7	4.3	2.5	3.0	2.7	3.1	2.7	2.6
Ba	564	614	590	583	564	515	664	684	713	210	192
La	34.4	33.7	41.1	34.3	35.8	33.6	39.1	43.1	32.7	26.0	25.9
Ce	68.5	75.2	75.0	72.0	74.2	70.7	75.1	82.6	65.5	53.1	52.4
Pr	8.78	8.48	10.2	8.37	8.60	8.69	9.23	10.5	7.84	5.00	6.44
Nd	32.5	30.8	37.8	30.2	31.0	31.5	33.5	37.1	29.1	24.0	23.8
Sm	6.58	5.98	7.46	5.78	5.89	5.94	6.05	6.66	5.43	4.96	5.00
Eu	1.45	1.41	1.71	1.36	1.31	1.19	1.16	1.31	1.23	0.86	0.91
Gd	6.12	5.64	6.57	5.54	5.55	5.39	5.46	5.52	4.95	4.40	4.76
Tb	0.847	0.787	0.982	0.769	0.760	0.760	0.770	0.857	0.769	0.685	0.733
Dy	4.70	4.28	5.39	4.29	4.24	4.37	4.50	4.90	4.67	3.86	4.35
Ho	0.98	0.88	1.09	0.86	0.85	0.87	0.93	1.02	0.98	0.80	0.89
Er	2.82	2.47	3.04	2.47	2.47	2.66	2.87	3.04	2.93	2.26	2.59
Yb	2.83	2.42	2.82	2.41	2.42	2.80	2.98	3.15	3.07	2.12	2.51
Lu	0.452	0.376	0.442	0.380	0.380	0.453	0.485	0.509	0.480	0.334	0.373
Hf	10.6	9.9	13.7	9.8	10.2	15.6	15.0	16.8	10.9	7.07	7.15
Ta	0.95	1.05	1.73	0.95	0.90	1.12	0.98	1.00	1.02	0.76	0.75
Th	11.0	13.0	11.0	11.8	12.2	11.4	11.8	13.2	10.8	7.95	8.45
U	2.75	3.03	3.11	2.74	2.82	2.91	3.13	3.12	2.85	2.59	2.93
La/Nb	3.0	3.0	2.3	2.9	3.2	2.4	2.5	2.9	2.2	2.6	2.7
Nb/Ta	12.2	10.7	10.2	12.9	12.6	12.5	16.1	15.1	14.8	13.1	12.7

| | Mt. Isa Group Shale | | | | State Circle Shale | | | | | | |
	MI 1	MI 2	MI 4	MI 5	SC 1	SC 2	SC 3	SC 4	SC 5	SC 7	SC 8
Ga	16.6	8.2	16.0	18.4	21.1	20.5	19.4	22.0	21.6	20.7	20.7
Sr	10.6	41.8	52.8	36.4	16.4	12.9	18.1	14.4	16.2	20.7	25.1
Y	8.82	20.4	20.8	18.8	22.8	31.9	25.4	24.3	20.3	27.9	22.1
Zr	93.6	91.2	129	198	144	146	161	146	133	133	137
Nb	10.1	6.89	12.0	14.2	14.4	14.8	14.3	14.5	14.6	14.0	14.1
Cs	4.6	3.6	7.9	13.6	7.8	9.4	6.6	8.4	9.6	9.1	7.8
Ba	274	25	276	240	369	258	293	495	408	349	332
La	20.3	38.6	33.4	33.2	28.1	41.1	29.7	43.5	24.5	44.2	32.8
Ce	34.0	77.1	71.3	78.6	62.8	84.2	63.4	89.8	63.5	88.7	75.5
Pr	4.61	8.44	7.67	7.72	7.29	10.0	7.08	10.2	6.70	10.3	8.41
Nd	16.2	29.8	26.4	27.5	30.0	36.2	27.9	37.2	24.5	37.0	32.2
Sm	2.85	5.25	4.89	4.89	6.07	7.30	5.61	7.67	4.84	4.97	6.59
Eu	0.51	0.76	0.82	0.87	1.31	1.45	1.12	1.48	0.92	0.90	1.07
Gd	2.32	4.40	4.20	4.13	5.93	7.54	5.95	5.95	4.31	4.27	5.19
Tb	0.32	0.60	0.63	0.61	0.75	0.99	0.79	1.00	0.65	0.64	0.81
Dy	1.81	3.25	3.55	3.50	4.48	5.42	4.32	5.35	3.74	3.68	4.71
Ho	0.37	0.69	0.73	0.72	0.93	1.12	0.95	1.05	0.76	0.77	0.98
Er	1.13	2.08	2.10	2.11	2.68	2.96	2.57	2.84	2.13	2.16	2.63
Yb	1.07	2.15	1.98	1.97	2.37	2.55	2.27	2.51	2.08	2.03	2.70
Lu	0.168	0.352	0.291	0.307	0.379	0.465	0.373	0.444	0.302	0.305	0.417

Table 2 (continued)

| | Mt. Isa Group Shale | | | | State Circle Shale | | | | | | |
	MI 1	MI 2	MI 4	MI 5	SC 1	SC 2	SC 3	SC 4	SC 5	SC 7	SC 8
Hf	2.85	2.64	3.60	5.47	4.09	4.43	4.90	4.21	4.01	3.90	4.09
Ta	0.78	0.61	0.99	1.19	1.43	1.42	1.39	1.41	1.22	1.11	1.19
Th	5.71	9.66	13.1	11.0	10.6	9.03	9.50	16.7	12.2	10.3	9.54
U	2.03	2.55	9.03	2.90	2.41	2.19	2.24	2.50	2.56	2.46	2.61
La/Nb	2.0	5.6	2.8	2.3	1.9	2.8	2.1	3.0	1.7	3.2	2.3
Nb/Ta	12.7	11.1	12.2	11.6	10.1	10.4	10.7	10.2	11.6	12.5	11.8

| | Perth Basin Shale | | | Canning Basin Shale | | Amadeus Basin Shale | | | | | |
	PW-4	PW-5	PW-7	PL-1	PL-6	AO 6	AO 7	AO 8	AO 9	AO 10	AO 12
Ga	28.4	27.1	22.9	22.2	19.7	19.2	19.7	17.5	19.3	21.3	23.9
Sr	96.0	86.4	63.4	43.9	218.4	60.1	74.6	66.7	37.6	64.7	60.8
Y	32.0	32.5	22.6	27.1	33.7	23.1	23.0	22.7	15.4	22.2	30.4
Zr	245	179	235	199	221	176	202	207	176	187	163
Nb	26.7	25.2	22.5	18.0	16.1	14.3	15.3	14.6	14.9	15.8	15.5
Cs	8.2	9.2	3.8	10.1	9.8	12.5	13.3	10.0	11.1	11.8	16.2
Ba	626	595	404	580	319	245	245	170	189	274	372
La	55.0	54.1	26.4	41.6	47.1	27.3	36.2	35.6	20.5	33.0	46.3
Ce	120	111	67.8	88.6	94.9	63.8	76.3	68.5	38.4	67.8	84.1
Pr	12.4	14.0	7.24	10.71	11.13	6.77	8.15	8.14	5.06	5.26	10.3
Nd	43.8	52.3	26.4	29.9	39.5	24.5	28.2	28.7	18.7	20.3	36.5
Sm	8.29	10.3	5.76	6.01	7.37	4.85	5.15	5.41	3.60	4.19	6.04
Eu	1.59	1.90	1.19	1.01	1.23	0.91	0.94	0.94	0.67	0.81	1.12
Gd	7.15	8.31	5.47	4.92	5.95	4.18	4.38	4.57	2.99	4.81	5.46
Tb	1.08	1.25	0.913	0.852	0.983	0.694	0.710	0.727	0.513	0.597	0.867
Dy	6.09	7.34	5.43	5.10	5.58	4.10	4.08	4.16	3.04	3.40	5.11
Ho	1.26	1.44	1.11	1.21	1.15	0.846	0.845	0.841	0.626	0.991	1.06
Er	3.65	4.02	3.22	3.56	3.36	2.45	2.52	2.43	1.88	2.79	3.04
Yb	3.54	3.66	2.99	3.49	3.19	2.42	2.50	2.31	1.87	2.50	3.01
Lu	0.531	0.557	0.443	0.499	0.478	0.366	0.382	0.355	0.287	0.407	0.444
Hf	6.81	5.08	6.95	5.71	5.72	4.90	5.55	5.73	4.98	5.46	4.51
Ta	1.88	1.90	1.69	1.44	1.37	1.14	1.24	1.16	1.22	1.27	1.19
Th	20.3	23.4	12.5	18.0	21.5	17.0	16.8	14.3	9.10	15.6	19.0
U	3.93	3.24	3.25	2.98	3.71	2.62	2.82	2.70	2.05	2.70	2.22
La/Nb	2.1	2.1	1.2	2.3	2.9	1.9	2.4	2.4	1.4	2.1	3.0
Nb/Ta	13.4	12.8	13.4	12.5	11.8	12.3	12.1	12.1	12.1	12.3	12.9

MHz (counts per second per ppm) for [115]In. Rinsing time and sample uptake time were set at 2 min and 5 min, respectively, in order to avoid the considerable memory effects observed for Ta. Free HF in the solutions required the use of a corrosion-resistant nebulizer (V-groove). The concentrations of Nb and Ta were further verified by standard addition experiments in selected samples. For the analytical setup described here, blank levels of 0.005 ppb Nb and 0.004 ppb Ta were determined by 8 measurements of blank solution. Detection limits of 0.020 ppb Nb and 0.007 ppb Ta were calculated at 3σ of signal variation of blank solution. At a dilution factor of 1/2500 for analysis, this results in detection limits of 0.050 ppm Nb and 0.018 ppm Ta for the samples, two orders of magnitude below the lowest observed abundances of 6.9 ppm Nb and 0.61 ppm Ta (shale sample MI 2). Long term external reproducibility is $\pm 3.5\%$ for Nb and $\pm 4.4\%$ for Ta (1σ) as determined by 11 measurements of the reference material GSP-1. Internal (within run) reproducibilities for these solutions are 2–3% (1σ).

4. Results

Trace element data for the loess and shale samples are given in Table 2. The loess samples show remarkably similar trace element patterns between different regions (Fig. 1) and within a specific region (Fig. 2, see also Fig. 3 in Taylor et al., 1983). Loess is highly enriched in large ion lithophile elements (LILE; e.g., Cs, Ba) and light REE relative to primitive mantle, with relatively flat heavy REE profiles and consistent negative Nb, Ta, and Ti anomalies relative to REE of similar incompatibilities. The Kaiserstuhl samples have lower absolute trace element abundances (but higher Sr) due to the diluting effect of their higher carbonate contents. In general, the trace element patterns resemble estimates of upper crustal composition. UCC-normalized trace element diagrams are shown in Fig. 2. The Sr depletion

seen in these samples is due to its solubility during continental weathering (e.g., Nesbitt et al., 1980), demonstrating that loess is derived from areas of moderate weathering (Gallet et al., 1998). Zr and Hf are enriched relative to upper crustal abundances, indicating that zircon is concentrated by the loess-forming process (Taylor et al., 1983). Nb and Ta are depleted relative to UCC (see below). The shales, although more heterogeneous than the loess samples, have similar trace element patterns to loess and UCC (Figs. 3 and 4). The shales show stronger Sr depletions, reflecting their higher degree of weathering compared to loess. Nb and Ta are depleted relative to UCC in the shales (except in the shales from the Perth Basin).

Our new trace element data show excellent agreement between ICP-MS and SSMS analyses for La and reasonable agreement for Nb. The average La
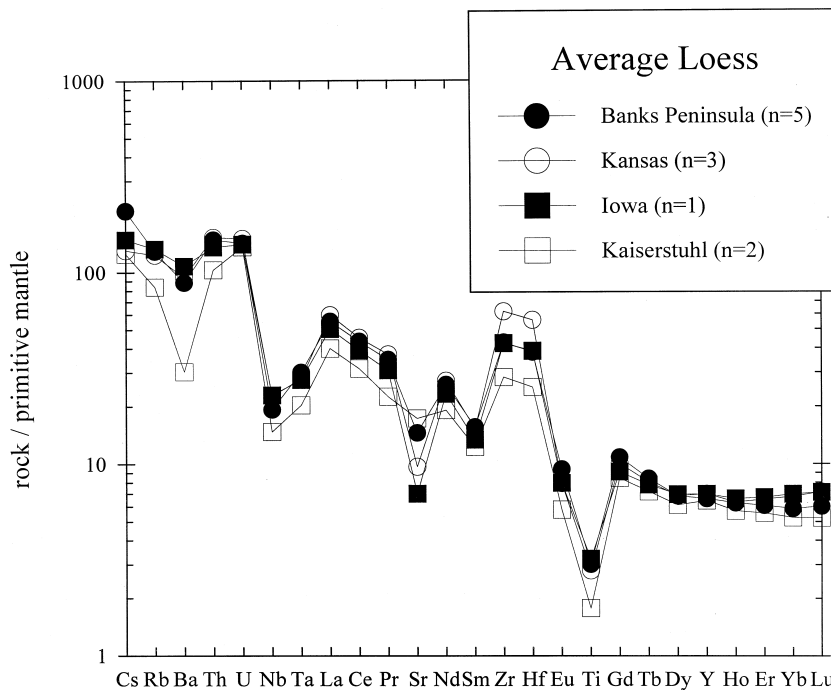
Fig. 1. Mantle-normalized diagram for incompatible elements in loess. Shown are the average values of loess samples from Banks Peninsula, New Zealand, Kansas and Iowa, USA, and Kaiserstuhl, Germany. The average values from different regions have very similar trace element patterns characterized by LILE and LREE enrichment, negative Nb-, Ta-, and Ti-anomalies, Zr and Hf enrichment and flat HREE. The trace element patterns of the Kaiserstuhl samples are nearly parallel to the other loess samples (except for Ba and Sr) but tend to have slightly lower abundances. This is best explained by dilution effects of carbonate minerals, which are abundant in these two samples but absent in the others. Element abundances are normalized to the primitive mantle values of McDonough and Sun (1995).
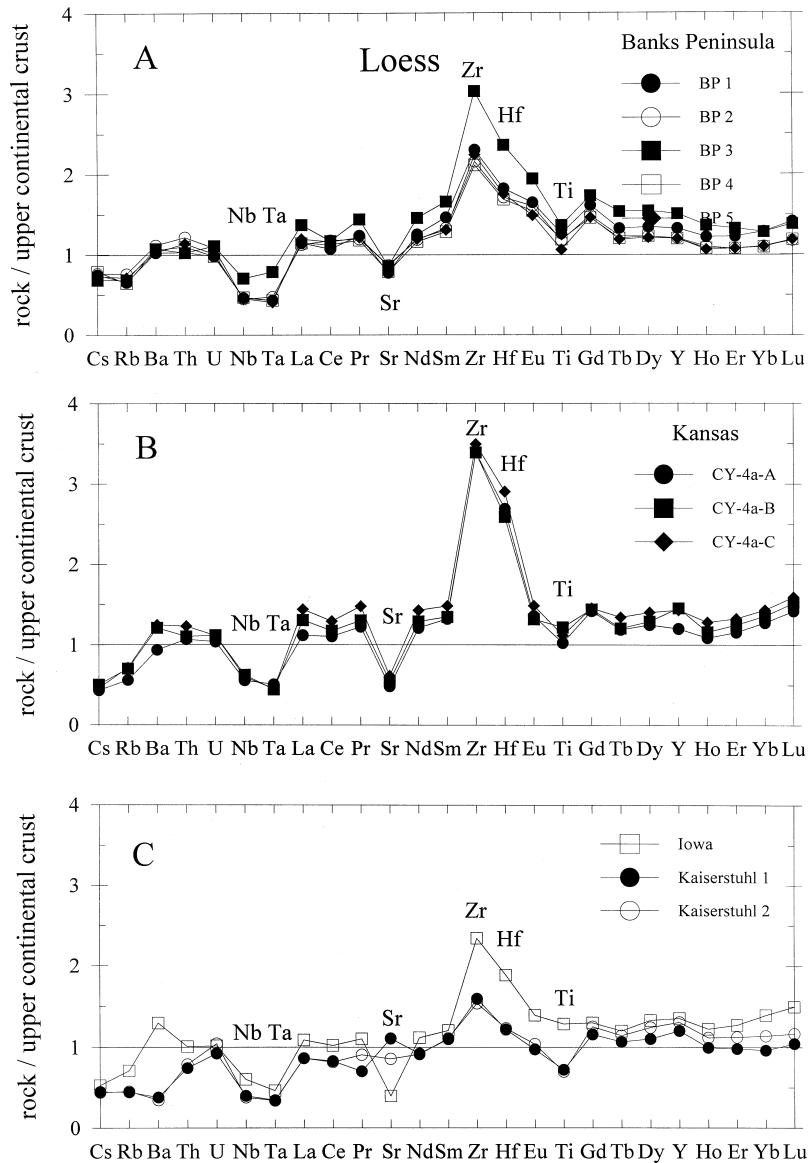
Fig. 2. Upper continental crust- normalized diagram for incompatible elements in loess. (A) Banks Peninsula, New Zealand. (B) Kansas, USA. (C) Iowa, USA and Kaiserstuhl, Germany. Element abundances are normalized to the upper crustal values of Taylor and McLennan (1985), except for Cs value from McDonough et al. (1992).

concentration of loess and PAAS and the average Nb concentration of PAAS agree between the two techniques to within 10% (Table 3). The average Nb concentration of loess determined by ICP-MS is ∼ 20% lower than the SSMS value (Table 3). For the individual samples, our La concentrations of the

loess samples and all but one of the values of Taylor et al. (1983) agree within 10%. The La concentration of sample CY-4a-B determined by ICP-MS is ∼ 25% higher than the SSMS value (39.1 ppm instead of 31 ppm). For half of the shale samples, our La concentrations and the values of Nance and Taylor (1976)
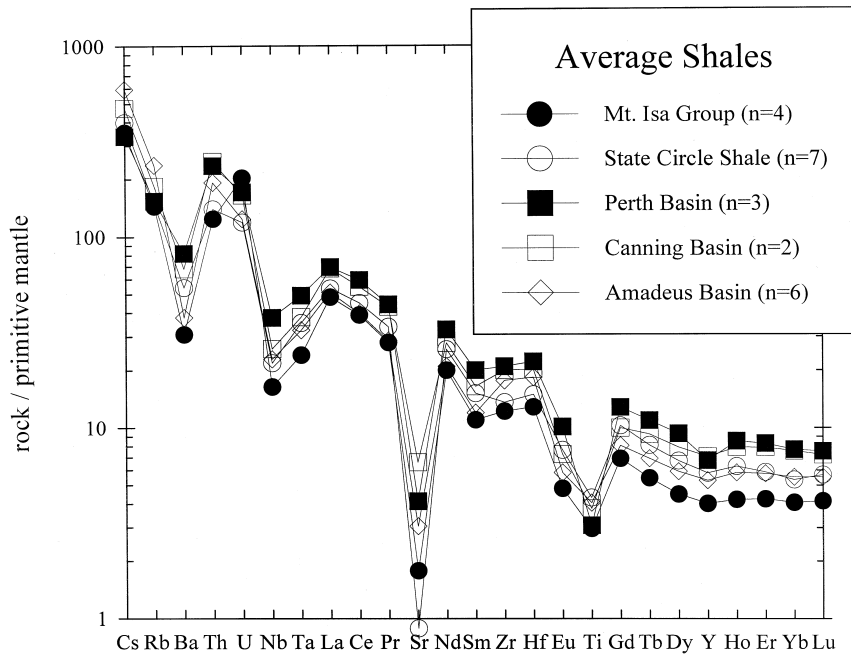
Fig. 3. Post-Archean Australian shales (normalized as in Fig. 1). Shown are the average values of four Middle Proterozoic shales from the Mt. Isa Group, seven Silurian State Circle shales, three Paleozoic to Mesozoic shales from the Perth Basin, two Paleozoic shales from the Canning Basin, and six Upper Proterozoic to Cambrian shales from the Amadeus Basin. Note the parallel nature of the patterns and the decreasing REE abundances with increasing age (see discussion in Nance and Taylor, 1976).

agree within 10%. Four shale samples show up to $\sim 30\%$ higher concentrations in comparison with the SSMS data; seven samples have up to $\sim 40\%$ lower concentrations. For six loess samples and eight shale samples, our Nb concentrations are up to $\sim 35\%$ lower than the SSMS values, e.g., the Nb concentration of sample BP-3 determined by ICP-MS is 17.6 ppm instead of 27 ppm determined by SSMS. Only one sample (shale SC 2) shows a significantly higher Nb concentration determined by ICP-MS (14.8 ppm instead of 12 ppm determined by SSMS).

Possible explanations for the discrepancies in La concentrations may be powder heterogeneity, i.e., fractionation of accessory REE-rich heavy minerals. Powder heterogeneity is supported by the observation that, for some samples, different digestions of the same sample resulted in different REE and Th contents, while other trace elements (e.g., Ga, Zr, Nb) showed the same concentrations. Enrichment or depletion of REE and Th suggests that small amounts of allanite or monazite are causing the sample het-

erogeneity (McLennan, 1989, and references therein). However, we do not consider sample heterogeneity to be an obstacle to the interpretation of our data since our average La concentration for PAAS is in excellent agreement with the average of Nance and Taylor (1976) (Table 3).

It is unlikely that the lower Nb values determined by ICP-MS are due to incomplete sample dissolution. Our own time series experiments have shown that zircon is more resistant to acid dissolution than Nb-bearing minerals (e.g., rutile and ilmenite) and only one sample (shale PL 1) shows lower Zr concentrations in comparison with the SSMS data. The higher SSMS values may be due to molecular interferences on ^{93}Nb ($^{29}Si^{16}O_4$ and $^{27}Al_3^{12}C$; Jochum et al., 1990) caused by the high concentrations of silica, aluminum, and carbon in the sample-graphite mixtures used during SSMS measurements. The sample preparation for ICP-MS (see above) effectively removes silica from the samples and, thus, greatly reduces consequent molecular interferences. Further-

more, the plasma ion source of the ICP-MS, unlike SSMS, also eliminates such complex polyatomic species in this mass region.

Our sediment samples have Nb, Ta, and La concentrations similar to other clastic sediments. The Nb, Ta, and La contents of our loess samples are nearly indistinguishable from loess from other regions (Pye and Johnson, 1988; Liu et al., 1993; Gallet et al., 1996, 1998). Oceanic sediments (Fig. 5) tend to have lower trace element concentrations due to the dilution of terrigenous material with biogenic, hydrothermal and hydrogenous components (Plank
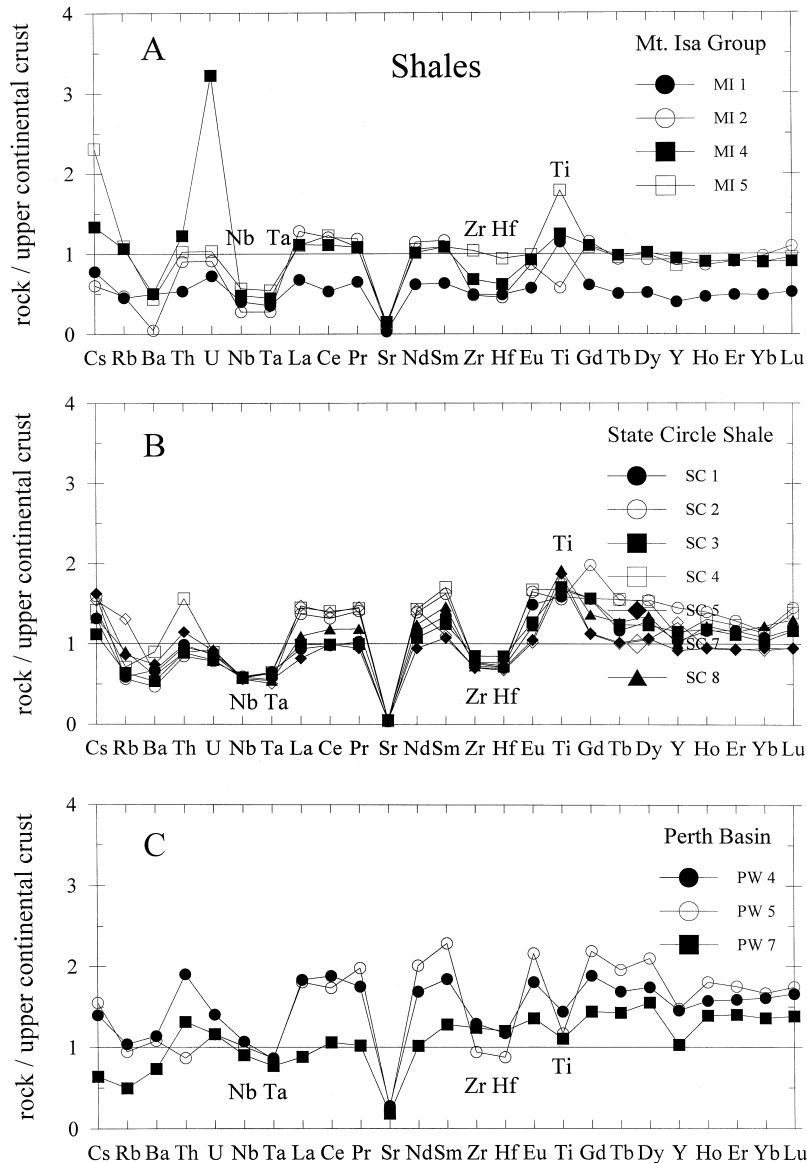
Fig. 4. Post-Archean Australian shales (normalized as in Fig. 2). (A) Middle Proterozoic shales from the Mt. Isa Group. (B) Silurian State Circle shale. (C) Paleozoic to Mesozoic shales from the Perth Basin. (D) Paleozoic shales from the Canning Basin. (E) Upper Proterozoic to Cambrian shales from the Amadeus Basin.
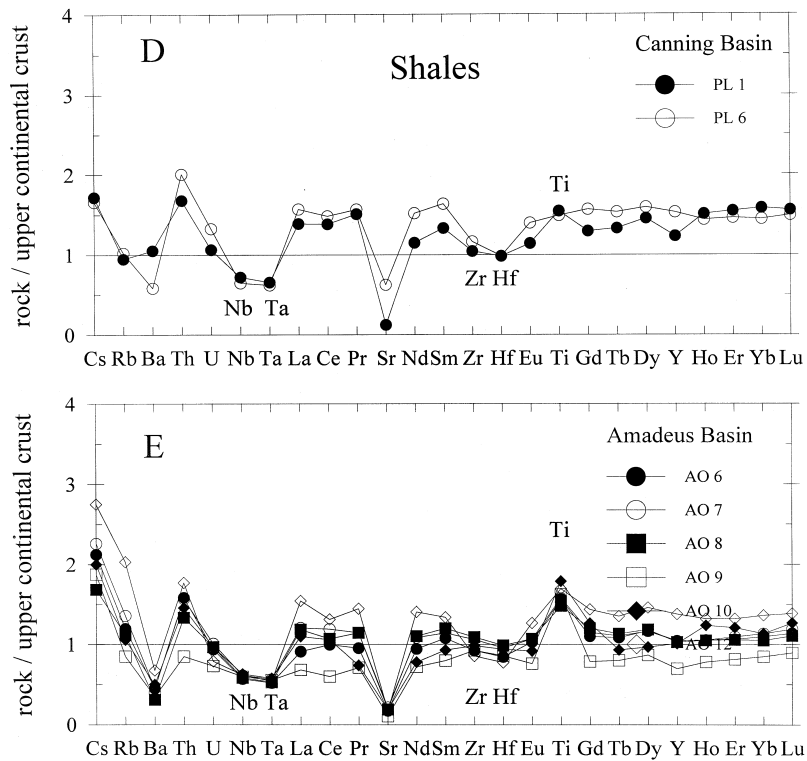
Fig. 4 (continued).

and Langmuir, 1998). The La concentrations of the loess and shale samples are about 20% higher than the estimate of Taylor and McLennan (1985) for the upper continental crust (TMUC, Table 2). If we decrease our numbers by 20%, as per Taylor and McLennan's arguments (see above), we find good

Table 3
Trace element concentrations of average loess, shales and the continental crust
Sources: Taylor et al. (1983), N + T = Nance and Taylor (1976) and McLennan (1981), G = Gao et al. (1998), T + M = Taylor and McLennan (1985), P + L = Plank and Langmuir (1998), R + F = Rudnick and Fountain (1995).

	Loess, this study	Loess, Taylor et al.	PAAS, this study	PAAS, N + T	East China, G
Nb (ppm)	13.0 ± 2.6	16.2 ± 5.8	15.6 ± 4.4	17.8 ± 5.4	12
Ta (ppm)	1.02 ± 0.26	–	1.28 ± 0.30	–	0.74
La (ppm)	35.0 ± 6.1	33.1 ± 4.9	38.4 ± 7.8	38.2 ± 8.3	34.8
Nb/Ta	12.9 ± 1.8	–	12.1 ± 1.1	–	16
La/Nb	2.7 ± 0.3	2.2 ± 0.6	2.6 ± 0.8	2.2 ± 0.4	2.9

	Upper crust, this study	Upper crust, T + M	Upper crust, P + L	Bulk crust, this study	Bulk crust, R + F
Nb (ppm)	11.5 ± 2.6	25	13.7 ± 0.9	8	12
Ta (ppm)	0.92 ± 0.12	2.2	0.96 ± 0.12	0.7	1.1
La (ppm)	30	30	30	18	18
Nb/Ta	12.5 ± 1.8	11.4	14.2 ± 1.8	12–13	11
La/Nb	2.6 ± 0.8	1.2	2.2	2.2	1.5
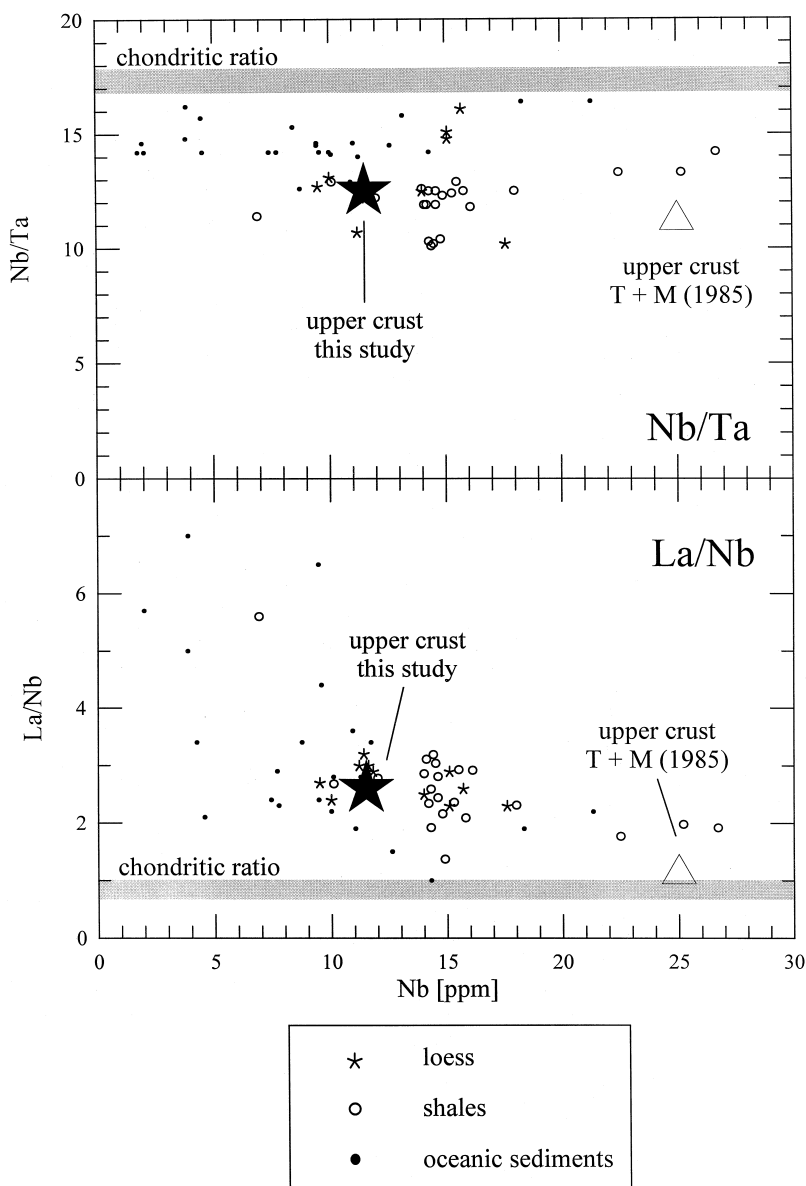
Fig. 5. Plot of Nb concentration vs. Nb/Ta ratio (upper panel) and La/Nb ratio (lower panel) for the loess (small stars) and shale (open circles) samples. Also shown are oceanic sediments (small dots; Plank and Langmuir, 1998), the chondritic ratios (gray bars; Jochum et al., 1997; McDonough and Sun, 1995), and the upper crustal values of this study (large star) and Taylor and McLennan (1985); open triangle. Note that the majority of the sediments have lower Nb concentrations and higher La/Nb than Taylor and McLennan's upper crustal estimate. All sediments show subchondritic Nb/Ta and superchondritic La/Nb.

agreement between Taylor and McLennan's upper crust and ours.

The loess samples and most of the shales have lower Nb concentrations than TMUC (Fig. 5) and show apparent negative Nb and Ta anomalies relative to TMUC (Figs. 2 and 4). It is unlikely that these anomalies are due to fractionation of heavy minerals (e.g., rutile) during transport of the sedi-

ments because we would expect Ti to show a similar depletion. However, the loess samples (except the Kaiserstuhl samples) and most of the shales have similar or higher Ti concentrations than TMUC. These observations suggest that the estimates of Nb and Ta for the UCC by Taylor and McLennan (1985) are too high. The estimate of the Nb concentration in TMUC (25 ppm; Taylor, 1977) is based on composite samples from the Canadian Shield (Shaw et al., 1976) (TMUC's Ta content is derived from an assumed Nb/Ta ratio of 11–12). Shaw et al.'s average value is not well established; the composite samples show large regional variation in concentration (4–50 ppm Nb) and several samples were below or very close to the detection limit of their XRF technique at that time. Our Nb concentrations are comparable to those reported for clastic sediments worldwide (e.g., Condie, 1993; Gallet et al., 1998) and agree with the estimate of Plank and Langmuir (1998) of the upper continental crust (PLUC, Table 3) based on global subducting oceanic sediment (GLOSS). The same trend holds true for Ta (Table 3). Our data support the revision in upper crust composition suggested by Plank and Langmuir (1998). Moreover, the estimate of Gao et al. (1998) of the upper crust in central East China, based on wide-scale sampling with analysis of composite samples, has a similarly high La/Nb (Table 3).

The Nb discrepancies also lead to differences in La/Nb of the upper crust. Our new data show that La/Nb increases to 2.7 ± 0.3 and 2.6 ± 0.8 for the loess and shale samples, respectively, leading to an even greater contrast between UCC and primitive mantle (1.0, McDonough and Sun, 1995). In order to obtain the upper crustal Nb concentration, we can either use our La/Nb ratio combined with the La value of Taylor and McLennan (1985) or decrease our Nb value by 20%, by analogy to the crustal La concentration. In both cases, we get 11.5 ± 2.6 ppm Nb, less than half of the Nb reported in TMUC.

Our average Nb/Ta ratios (12.9 ± 1.8 for loess and 12.1 ± 1.1 for shales) agree within uncertainty with both TMUC (11–12) and GLOSS (14.2 ± 1.8). All of our Nb/Ta values are significantly lower (10.1–16.1) than the chondritic value (17.4 ± 0.5; Jochum et al., 1997). The crustal Ta concentration of 0.92 ± 0.12 ppm is calculated from our average Nb/Ta = 12.5 ± 1.8. Both Nb and Ta are lower than

the estimate of Plank and Langmuir (1998) of the upper continental crust but they agree within error, which is remarkable because Plank and Langmuir's and our crustal estimates are derived from different and independent sample sets. Plank and Langmuir's estimate is based on marine sediments that (1) have a complex history of weathering, transport, and marine deposition in comparison with terrigeneous sediments and (2) do not include samples from the Atlantic Ocean, i.e., its sample set excludes detrital material derived from eastern North America and Europe, where many of the loess samples originate.

5. Discussion

When we apply our Nb and Ta values for the upper crust to the recent estimate of the bulk continental crust of Rudnick and Fountain (1995), both Nb and Ta concentrations decrease by $\sim 30\%$, leading to Nb = 8 ppm (instead of 12) and Ta = 0.7 ppm (instead of 1.1). La/Nb of the bulk crust increases from 1.5 to 2.2, only slightly higher than the estimate of Plank and Langmuir (1998). These revisions lead to Nb/U = 5.6 (instead of 8.5) and, thus, to an even greater contrast between the continental crust and the oceanic mantle (47 ± 10; Hofmann et al., 1986) for this element ratio.

Both the crustal Nb/Ta ratio and the increased crustal La/Nb ratio support the observation that the continental crust and the Depleted Mantle are not complementary silicate reservoirs with respect to La, Nb, and Ta (Fig. 6; Sun and McDonough, 1989; McDonough, 1991). Both the continental crust (Plank and Langmuir, 1998; this study) and the Depleted Mantle (Jochum et al., 1997; Niu and Batiza, 1997) have subchondritic Nb/Ta and superchondritic La/Nb. These trace element ratios support the suggestion of a Nb- and Ta-rich reservoir within the Earth having high Nb/Ta and low La/Nb. There are several implications of these observations. Firstly, the Nb/U ratio cannot be used to model crust–mantle differentiation with simple two-reservoir models which assume that the continental crust and the Depleted Mantle are complementary to one another (cf. Hofmann et al., 1986; Sylvester et al., 1997). Secondly, in order to balance the Silicate Earth,
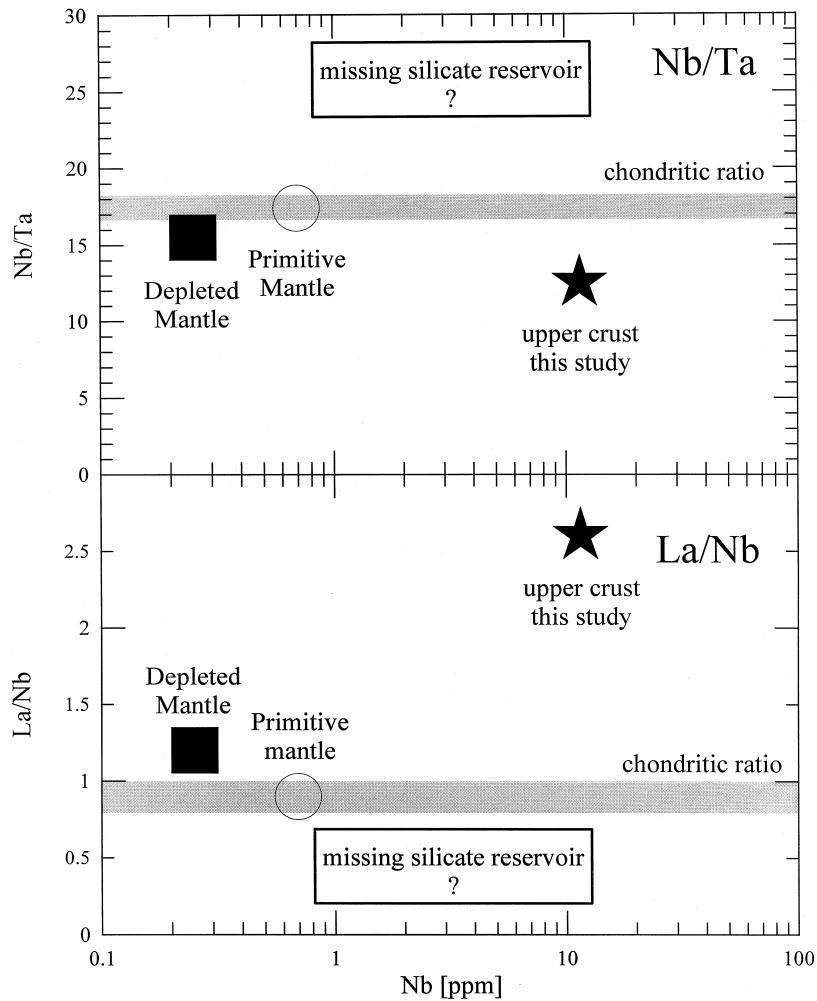
Fig. 6. Plot of Nb concentration vs. Nb/Ta ratio (upper panel) and La/Nb ratio (lower panel) for the chondritic ratios (gray bars; McDonough and Sun, 1995; Jochum et al., 1997), primitive mantle (open circle), depleted mantle (solid square; Jochum et al., 1998), and the upper crustal value of this study (solid star). Also shown is an estimate of a possible Nb-rich reservoir required to balance Nb and Ta in the Silicate Earth (McDonough, 1991; Jochum and Hofmann, 1998; Rudnick et al., 1998). Note the logarithmic scale of the Nb concentration. Both the depleted mantle and the continental crust have subchondritic Nb/Ta and superchondritic La/Nb, indicating that depleted mantle and continental crust are not complementary reservoirs with respect to Nb and Ta. Thus, an additional Nb- and Ta-rich reservoir having superchondritic Nb/Ta is required to balance the Silicate Earth, supporting the suggestion of sequestered eclogite in the deep earth.

McDonough (1991) proposed a refractory rutile-bearing eclogite reservoir exists (~ 2% by mass of the Silicate Earth) that is sequestered deep in the mantle. Our recent analysis of eclogite xenoliths supports the contention that refractory rutile-bearing eclogite, presumably formed through subduction of mafic oceanic crust, does indeed solve the Nb–Ta–La mass balance problem (Rudnick et al., 1998).

It has been proposed that the continental crust's La/Nb can be used to place constraints on the proportion of crust formed in intraplate vs. convergent margin settings (Rudnick, 1995). This is because intraplate magmas have La/Nb generally < 1.0 (Sun and McDonough, 1989) whereas convergent margin magmas typically have high La/Nb ratios (e.g., McCulloch and Gamble, 1991, and refer-

ences therein). Mixing between average arc basalts and possible intraplate basalts is illustrated in Fig. 7. This mixing scenario assumes that the crust grows by basalt addition. The higher La/Nb ratio of the crust suggested here and by Plank and Langmuir (1998) implies a lower contribution of intraplate
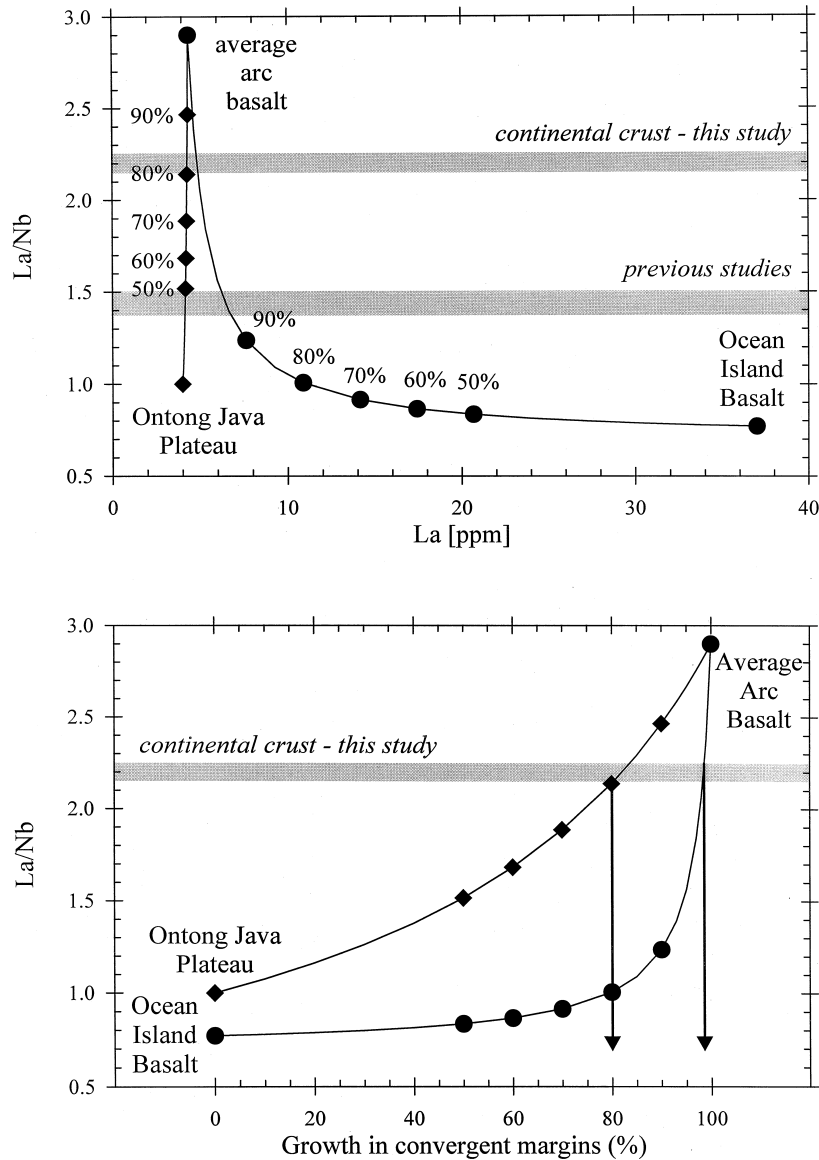

Fig. 7. Mixing relationships between average arc basalt (McCulloch and Gamble, 1991) and intraplate magmas (Sun and McDonough, 1989; Neal et al., 1997). The upper panel shows a plot of the La concentration vs. the La/Nb ratio. Diamonds and circles represent 10% increments. Continental crust bars represent range of ratios from estimates of previous studies (Taylor and McLennan, 1985; Gao et al., 1992; Rudnick and Fountain, 1995; Wedepohl, 1995) and this study. The lower panel shows a plot of the proportion of the convergent margin component vs. the La/Nb ratio. Horizontal bar represents an estimated average value for the continental crust. Where it intersects the mixing lines, the percentage of intraplate component can be read from the x-axis (marked by arrows). Note that the La/Nb ratio of this study (solid arrows) results in a smaller percentage of intraplate component than previous estimates. Modified from Rudnick (1995).

magmas to the growth of the continental crust. The calculation is not very sensitive to the composition of the convergent margin component: we found our own average arc basalt taken from our literature compilation is indistinguishable from that of McCulloch and Gamble (1991). However, the proportion of intraplate component needed to explain the crustal La/Nb ratio depends strongly on its composition. If the intraplate component has high trace element concentrations (average ocean island basalt, Sun and McDonough, 1989), less than 5% is sufficient. Alternatively, the continental crust could accommodate about 20% of an intraplate component with low trace element concentrations, e.g., the Ontong Java Plateau basalts (Neal et al., 1997).

While this mixing calculation is able to reproduce the La/Nb ratio, it fails to account for the evolved bulk composition of the continents. Three different processes may explain the intermediate composition of the continents, as reviewed in Rudnick (1995). (1) Direct addition of silicic melts of tonalitic–trondhjemitic–granodioritic (TTG) composition with subduction of the complementary rutile-bearing mafic oceanic crust (e.g., Martin, 1986). (2) Intracrustal differentiation of basaltic crust to form evolved melts and the subsequent delamination of parts of the mafic to ultramafic residues (e.g., Arndt and Goldstein, 1989; Kay and Kay, 1991). (3) Chemical weathering of surface rocks drives the crust to more evolved compositions by preferential recycling of Mg to mantle (e.g., Anderson, 1982; Albarède, 1998).

How might these processes affect the La/Nb ratio of the bulk crust? The first process would increase La/Nb and be inherently a convergent margin process. Process 2 could drive the crust to higher La/Nb if the delaminated residue has subchondritic La/Nb. La/Nb decreases with depth in the continental crust, but it never reaches the chondritic value (Rudnick and Fountain, 1995). So, although delamination is expected to increase the bulk crust La/Nb, it is unlikely to have produced the superchondritic La/Nb in the first place. Finally, chemical weathering (process 3) does not change La/Nb because both La and Nb are immobile (see above).

Thus, although the mixing calculation shown in Fig. 7 is clearly an oversimplification, the main conclusion, that the crust is primarily a product of convergent margin magmatism, is robust.

6. Conclusions

Our new data for the classic loess and shale (PAAS) samples of Taylor and McLennan lead to the following conclusions.

The upper continental crust has average Nb = 11.5 ppm and Ta = 0.92 ppm, which translates into a bulk crust Nb = 8 ppm, Ta = 0.7 ppm, La/Nb = 2.2, and Nb/Ta = 12–13.

The subchondritic Nb/Ta and Nb/La in both continental crust and Depleted Mantle demonstrate that these reservoirs are not strictly complementary with respect to La, Nb, and Ta and supports the suggestion of a Nb-rich eclogitic reservoir sequestered in the deep earth (McDonough, 1991).

The higher La/Nb suggests an even lower plume contribution to the continents — 5–20% — than estimated by Rudnick (1995).

References

Albarède, F., 1998. The growth of continental crust. Tectonophysics 296, 1–14.

Anderson, A.T. Jr., 1982. Parental basalts in subduction zones: implications for continental evolution. J. Geophys. Res. 87, 7047–7060.

Arndt, N.T., Goldstein, S.L., 1989. An open boundary between lower continental crust and mantle: its role in crust formation and crustal recycling. Tectonophysics 161, 201–212.

Condie, K.C., 1993. Chemical composition and evolution of the upper continental crust: contrasting results from surface samples and shales. Chem. Geol. 104, 1–37.

Eggins, S.M., Woodhead, J.D., Kinsley, L.P.J., Mortimer, G.E., Sylvester, P., McCulloch, M.T., Hergt, J.M., Handler, M.R., 1997. A simple method for the precise determination of ≥ 40 trace elements in geological samples by ICPMS using enriched isotope internal standardisation. Chem. Geol. 134, 311–326.

Flint, R.F., 1971. Glacial and Quaternary Geology. Wiley, New York, 892 pp.

Gallet, S., Jahn, B.-M., Torii, M., 1996. Geochemical characterization of the Luochuan loess-paleosol sequence, China, and paleoclimatic implications. Chem. Geol. 133, 67–88.

Gallet, S., Jahn, B.-m., van Vliet Lanoë, B., Dia, A., Rossello, E., 1998. Loess geochemistry and its implications for particle origin and composition of the upper continental crust. Earth Planet. Sci. Lett. 156, 157–172.

Gao, S., Zhang, B.R., Luo, T.C., Li, Z.J., Xie, Q.L., Gu, X.M., Zhang, H.F., Ouyang, J.P., Wang, D.P., Gao, C.L., 1992. Chemical composition of the continental crust in the Qinling orogenic belt and its adjacent North China and Yangtze cratons. Geochim. Cosmochim. Acta 56, 3933–3950.

Gao, S., Luo, T.-C., Zhang, B.-R., Zhang, H.-F., Han, Y.-W., Zhao, Z.-D., Hu, Y.-K., 1998. Chemical composition of the continental crust as revealed by studies in East China. Geochim. Cosmochim. Acta 62, 1959–1975.

Govindaraju, K., 1994. 1994 compilation of working values and sample description for 383 geostandards. Geostand. Newslett. 18, 1–158.

Hall, G.E.M., Plant, J.A., 1992. Analytical errors in the determination of high field strength elements and their implications in tectonic interpretation studies. Chem. Geol. 95, 141–156.

Hofmann, A.W., 1988. Chemical differentiation of the Earth: the relationship between mantle, continental crust, and oceanic crust. Eart Planet. Sci. Lett. 90, 297–314.

Hofmann, A.W., Jochum, K.P., Seufert, M., White, W.M., 1986. Nb and Pb in oceanic basalts: new constraints on mantle evolution. Earth Planet. Sci. Lett. 79, 33–45.

Jenner, G.A., Longerich, H.P., Jackson, S.E., Fryer, B.J., 1990. ICP-MS — A powerful tool for high-precision trace-element analysis in Earth sciences: evidence from analysis of selected U.S.G.S. reference samples. Chem. Geol. 83, 133–148.

Jochum, K.P., Hofmann, A.W., 1998. Nb/Ta in MORB and continental crust: implications for a superchondritic Nb/Ta reservoir in the mantle. EOS (Trans. Am. Geophys. Union) 79, S354.

Jochum, K.P., Seufert, H.M., Thirlwall, M.F., 1990. High-sensitivity Nb analysis by spark-source mass spectrometry (SSMS) and calibration of XRF Nb and Zr. Chem. Geol. 81, 1–16.

Jochum, K.P., Pfänder, J., Snow, J.E., Hofmann, A.W., 1997. Nb/Ta in mantle and crust. EOS (Trans. Am. Geophys. Union) 78, 804.

Jochum, K.P., Hofmann, A.W., Pfänder, J., 1998. Constraints on the abundances and abundance ratios of Nb, Ta, Th and U in the Earth's mantle and crust using high precision MIC-SSMS data. GERM Workshop La Jolla, pp. 45–47.

Kay, R.W., Kay, S.M., 1991. Creation and destruction of lower continental crust. Geol. Rundschau 80, 259–278.

Liu, C.-Q., Masuda, A., Okada, A., Yabuki, S., Zhang, J., Fan, Z.-L., 1993. A geochemical study of loess and desert sand in northern China: implications for continental crust weathering and composition. Chem. Geol. 106, 359–374.

McCulloch, M.T., Gamble, A.J., 1991. Geochemical and geodynamical constraints on subduction zone magmatism. Earth Planet. Sci. Lett. 102, 358–374.

McDonough, W.F., 1991. Partial melting of subducted oceanic crust and isolation of its residual eclogitic lithology. Philos. Trans. R. Soc. Lond. A 335, 407–418.

McDonough, W.F., Sun, S.-S., 1995. Composition of the Earth. Chem. Geol. 120, 223–253.

McDonough, W.F., Sun, S.-S., Ringwood, A.E., Jagoutz, E., Hofmann, A.W., 1992. Potassium, rubidium, and cesium in the Earth and Moon and the evolution of the mantle of the Earth. Geochim. Cosmochim. Acta 56, 1001–1012.

Martin, H., 1986. Effect of steeper Archean geothermal gradient on geochemistry of subduction-zone magmas. Geology 14, 753–756.

McLennan, S.M., 1981. Trace element geochemistry of sedimentary rocks: implications for the composition and evolution of the continental crust. Ph.D. thesis, Australian National University.

McLennan, S.M., 1989. Rare earth elements in sedimentary rocks: influence of provenance and sedimentary processes. In: Lipin, B.R., McKay, G.A. (Eds.), Geochemistry and Mineralogy of Rare Earth Elements. Mineral. Soc. Am., Washington, DC, pp. 169–200.

Münker, C., 1998. Nb/Ta fractionation in a Cambrian arc/back arc system, New Zealand: source constraints and application of refined ICPMS techniques. Chem. Geol. 144, 23–45.

Nance, W.B., Taylor, S.R., 1976. Rare earth element pattern and crustal evolution: I. Australian post-Archean sedimentary rocks. Geochim. Cosmochim. Acta 40, 1539–1551.

Neal, C.R., Mahoney, J.J., Kroenke, L.W., Duncan, R.A., Petterson, M.G., 1997. The Ontong Java Plateau. In: Mahoney, J.J., Coffin, M.F. (Eds.), Large Igneous Provinces: Continental, Oceanic, and Planetary Flood Volcanism. AGU, Washington, DC, pp. 183–216.

Nesbitt, H.W., Markovics, G., Price, R.C., 1980. Chemical processes affecting alkalis and alkaline earths during continental weathering. Geochim. Cosmochim. Acta 44, 1659–1666.

Niu, Y., Batiza, R., 1997. Trace element evidence from seamounts for recycled oceanic crust in the eastern Pacific mantle. Earth Planet. Sci. Lett. 148, 471–483.

Owen, L.B., Faure, G., 1974. Simultaneous determination of Hafnium and Zirconium in silicate rocks by isotope dilution. Anal. Chem. 46, 1323–1326.

Plank, T., Langmuir, C.H., 1998. The chemical composition of subducting sediment and its consequences for the crust and mantle. Chem. Geol. 145, 325–394.

Pye, K., Johnson, R., 1988. Stratigraphy, geochemistry, and thermoluminescence ages of Lower Mississippi Valley loess. Earth Surf. Process. Landforms 13, 103–124.

Rudnick, R.L., 1995. Making continental crust. Nature 378, 571–578.

Rudnick, R.L., Fountain, D.M., 1995. Nature and composition of the continental crust: a lower crustal perspective. Rev. Geophys. 33, 267–309.

Rudnick, R.L., Barth, M.G., McDonough, W.F., Horn, I., 1998. Rutiles in eclogites: a missing Earth reservoir found? GSA Abstr. 30 (7), A–207, Toronto.

Shaw, D.M., Dostal, J., Keays, R.R., 1976. Additional estimates of continental surface Precambrian Shield composition in Canada. Geochim. Cosmochim. Acta 40, 73–83.

Smalley, I.J., Vita-Finzi, C., 1968. The formation of fine particles

in sandy deserts and the nature of 'desert' loess. J. Sediment. Petrol. 38, 766–775.

Sun, S.-S., McDonough, W.F., 1989. Chemical and isotopic systematics of oceanic basalts; implications for mantle composition and processes. In: Saunders, A.D., Norry, M.J. (Eds.), Magmatism in the Ocean Basins, Geol. Soc. Lond. Spec. Pub. 42, 313–345.

Sylvester, P.J., Campbell, I.H., Bowyer, D.A., 1997. Niobium/Uranium evidence for early formation of the continental crust. Science 275, 521–523.

Taylor, S.R., 1977. Island arc models and the composition of the continental crust. In: Talwani, M., Pitman, W.C., III (Eds.), Island Arcs, Deep Sea Trenches and Back-Arc Basins. AGU, Washington, DC, pp. 325–335.

Taylor, S.R., McLennan, S.M., 1985. The Continental Crust: Its Composition and Evolution. Blackwell, Oxford, 312 pp.

Taylor, S.R., McLennan, S.M., McCulloch, M.T., 1983. Geochemistry of loess, continental crustal composition and crustal model ages. Geochim. Cosmochim. Acta 47, 1897–1905.

Totland, M., Jarvis, I., Jarvis, K.E., 1992. An assessment of dissolution techniques for the analysis of geological samples by plasma spectrometry. Chem. Geol. 95, 35–62.

Wedepohl, K.H., 1995. The composition of the continental crust. Geochim. Cosmochim. Acta 59, 1217–1232.

Xie, Q., Jain, J., Sun, M., Kerrich, R., Fan, J., 1994. ICP-MS analysis of basalt BIR-1 for trace elements. Geostand. Newslett. 18, 53–63.